Electronic Supplementary Material (ESI) for Physical Chemistry Chemical Physics.

Electronic Supplementary Information:

Collision induced charge separation in ground-state water splitting dynamics

Kentaro Yamamoto* and Kazuo Takatsuka†
Fukui Institute for Fundamental Chemistry, Kyoto University,
Takano-Nishihiraki-cho 34-4, Sakyou-ku, Kyoto 606-8103, Japan

April 2, 2018

Contents

---

*email: `kyamamoto@fukui.kyoto-u.ac.jp`
†email: `kaztak@fukui.kyoto-u.ac.jp`

S1 Repulsive nature between EA1$^+$ and EA2–H^1

As mentioned in the main text, EA1$^+$ (EA1 = electron acceptor 1: semiquinone) and EA2–H^1 (EA2 = electron acceptor 2: 4-methylphenoxyl group) are repulsive to each other at the given configuration, in which the benzene rings are placed on the same plain and four substituents are aligned on the same line. Geometry optimization has been carried out starting from the other configurations such as stacking fashion usually let EA1$^+$ hydrogen-bond to either PA (proton acceptor: imidazole) or EPD–H^3 (EPD = electron–proton donor: Mn(OH)$_2$). However, they do not necessarily lead to the reaction under the present mechanism, because appropriate timing and molecular orientation are not given. A configurational restriction to find the mechanism seems to be rather artificial, but it is needed to keep the size of super molecular system moderate enough to allow us to perform the calculation of the full-dimensional nonadiabatic electron dynamics. We here demonstrate the repulsive nature between the two species EA1$^+$ and EA2 in the given initial condition (the hole is localized in EA1$^+$) by using relevant potential energy curves. In addition, similar potential curves for the states in which the hole is localized in either EA2 and EPD to show that EA1 and EA2 are still not of strong attractive nature at all.

S1.1 The three key states

Three key states are prepared so that each of them represents a typical point of nonadiabatic electron dynamics. They are referred to as State 1, State 2, and State 3, which have a hole in EA1, EA2, or EPD, respectively. The molecular configurations are represented as follows

$$\begin{cases} \text{State 1}: & \text{EA1}^+,\ \text{EA2–H}^1(\cdots\text{PA})\cdots\text{H}^2\text{–W},\ \text{H}^3\text{–EPD} & (t = 0\ \text{fs}) \\ \text{State 2}: & \text{EA1}^\bullet,\ \text{EA2}^\bullet\cdots(\text{H}^1\text{–PA}^+)\cdots\text{H}^2\text{–W},\ \text{H}^3\text{–EPD} & (t = 9\ \text{fs}) \\ \text{State 3}: & \text{EA1}^\bullet,\ \text{EA2–H}^2(\cdots\text{H}^1\text{–PA}^+)\cdots\text{W–H}^3\cdots\text{EPD}^\bullet & (t = 147\ \text{fs}) \end{cases} \tag{1}$$

The timings of dynamics are also given in eqn (1). See Figure 3 in the main text. State 1 is obtained in almost the same way as the preparation of initial condition. First we separately optimize the EA1$^+$ and EA2–H^1($\cdots$PA)$\cdots$H^2–W$\cdots$H^3–EPD. And then EA1$^+$ is placed on the same plain as mentioned above. Finally, The parallel translation of EPD–H^3 is performed along the line connecting the O atom of water molecule (W) and the nearer O of EPD up to 4.5 Å in the OO distance to extend the EPD–W distance. State 2 is prepared similarly to the State 1, but EA1$^\bullet$ and EA2$^\bullet\cdots$(H^1–PA$^+$)$\cdots$H^2–W$\cdots$H^3–EPD are used instead. State 3 is prepared similarly by using EA1$^\bullet$ and EA2–H^2($\cdots$H^1–PA$^+$)$\cdots$W–H^3. Note that EPD translation is not performed in State 3, because this state is supposed to be obtained after the EPD–EA2 collision.

S1.2 Potential energy curves as functions of the EA1–EA2 distance

The potential energy curves are calculated as functions of the distance of EA1 and EA2 that is represented as the CO distance, in which C and O are from the methyl group of EA2 and the nearer O atom of EA1, respectively. As shown in Figure S1a, EA1$^+$ and EA2–H^1 is indeed repulsive to each other in State 1. We found from the preliminary short-time dynamics calculations that the nonadiabatic interaction becomes significantly strong when the CO distance is lower than 2.5 Å. Thus some external force is needed to realize an efficient electron transfer, because the potential energy curve of the ground state is no longer flat in such a region. On the other hand, in State 2 (Figure S1b), EA1$^\bullet$ and EA2$^\bullet$ turns to be slightly attractive. However, this may not be deep enough to keep the EA1 around EA2 after the first collision in the present conditions, if the system undergoes EA1$^+$ ←EA2 electron transfer, because they need to approach each other to a distance shorter than approximately 2.5 Å by collision. EA1$^\bullet$ is indeed not caught by EA2$^\bullet$ in our dynamical calculations (see Figure 2, for example). In State 3 (Figure S1c), EA1$^\bullet$ and EA2–H^1 is less attractive than those of State 2. Consequently, the chance of the electron transfer of EA1→EA2 (reverse) is suppressed by the EA2←EPD electron transfer.

S2 On the level of quantum chemical calculations

In our studies, the model system and the level of quantum chemical calculations have been chosen so that they qualitatively describe fundamental chemical mechanisms. Among others, the choices of atomic basis sets and CI active spaces are particularly is vital to determine the absolute value of the energy and structures. However, it turns out that the fundamental chemical mechanisms we found does not strongly depend on the choice of the level of calculation. This is partly because nonadiabatic electron wavepacket dynamics can grasp the essential feature of chemistry. [1, 2] But its applications in higher accuracy remain challenging to us. For this reason, we first try to find the fundamental mechanisms with simplest possible system and the level of calculation has been made higher as much as we could. We herein focus on the atomic basis set and the CI active space, and show that the present mechanism probably remains the same even if the higher level of calculation is employed.

S2.1 Polarization and diffuse functions in an atomic basis set

The atomic basis set employed for the atoms other than Mn is 6-31G in the present work, that is, no polarization and diffuse functions are included. Here the ground electronic states of the key three states having a hole in EA1, EA2, or EPD, which are obtained by the same manner as Section S1.1 with a different atomic basis set. The CO distance (EA1–EA2 distance) is set to be 2.5 Å, when a hole is localized in EA1 or EA2 and 5.5 Å, and when it is in EPD to reflect the situation of the dynamical result. We compare the cases with and without polarization and diffuse functions for C, N, and O atoms. Those for H and Mn remain the same. In short, the results of 6-31G (the present choice) and 6-31+G* basis sets are compared. The CISD active space is chosen to be the same, namely, (HOMO−67) – LUMO for the sake of simplicity.

As shown in Figure S2, qualitatively the same geometry and electronic states are obtained even the polarization and diffuse functions are added. Thus the mechanism itself would be robust with respect to the quality of atomic basis set chosen. However, the relative energy of the state with the hole in EPD would be underestimated as much as 1 eV.

In our previous studies on the excited-state CPEWT [3–6], diffuse functions in the atomic basis set have played critical roles, because the destination of transferred electron is commonly the dense manifold of Rydberg-like states mainly centered at nitrogen atoms. In these cases, the diffuse functions are by far indispensable. In the present study, on the other hand, the destination of electron is the π states of either semiquinone or 4-methylphenol, in which diffuse orbitals are not as critical as in the photoexcited dynamics, although the relative energy levels of the relevant systems are affected rather quantitatively as seen in Fig. S2.

Incidentally, it takes 7 - 8 times more computational cost by adding the polarization and diffuse orbitals in the atomic basis set, which actually prevents our practical calculations in the present level of full dimensional electron and nuclear dynamics.

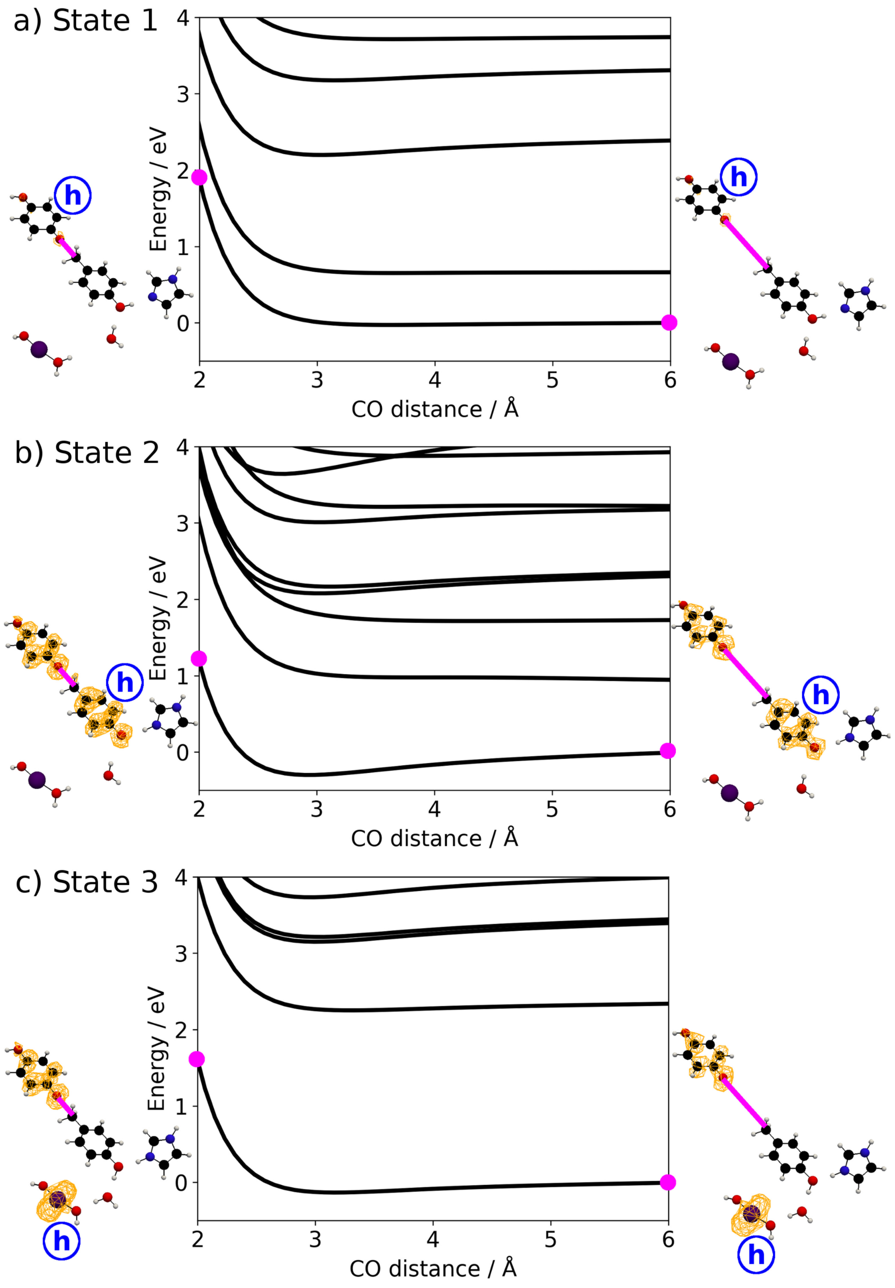

Figure S1: Potential energy curves relevant to the EA1–EA2 detachment for (a) State 1, (b) State 2, and (c) State 3. The terminal structures for each key state are given at each side. Spatial distribution of unpaired electron density is expressed as orange iso-surface, and the hole positions are indicated by "h". The CO distance is indicated by the pink line given for each super molecule.

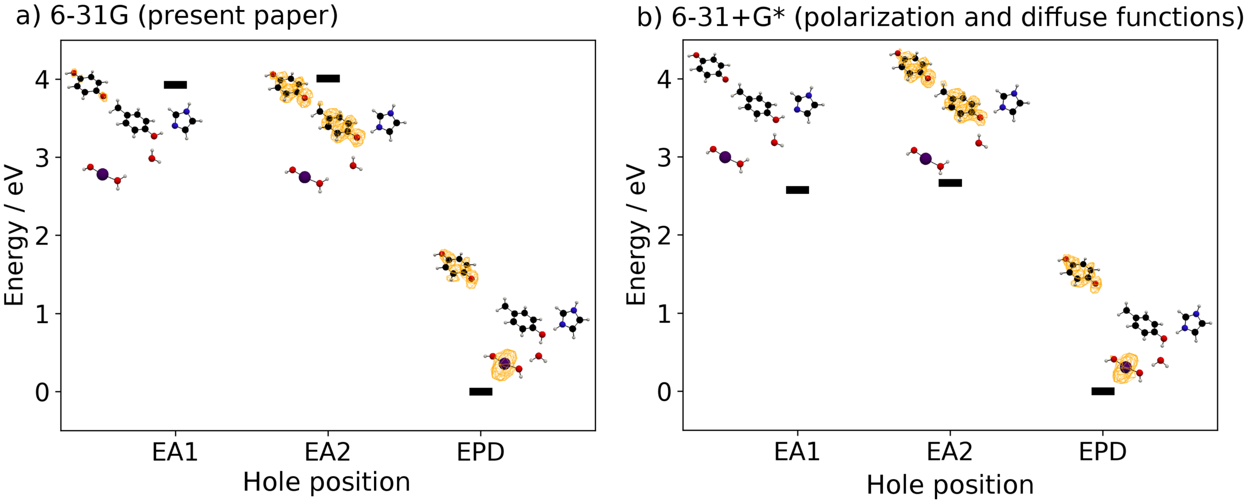

Figure S2: Comparison of the electronic states (represented by the spatial distribution of unpaired electron density) and their energy by using a different atomic basis set for three key structures in which the hole is in EA1$^+$, EA2, or EPD. The atomic basis set for C, N, and O atoms are varied for comparison. (a) 6-31G basis that is used as in the present study. (b) 6-31+G* basis set (including diffuse and polarization functions).

Table S1: Comparison of the total electronic energy and dominant configurations for different CISD active spaces for the three key structures. The base of energy is set to be -34,800 eV. "Coef." and "Occ." stand for CI coefficients and MO occupancy for dominant states, respectively. MO occupation is only given for HOMO−1, HOMO, and LUMO and all other MOs are doubly occupied (HOMO−1 and lower) or virtual (LUMO+1 and higher).

	(HOMO−67) – LUMO			(HOMO−4) – (LUMO+14)		
Hole	Energy/eV	Coef.	Occ.	Energy/eV	Coef.	Occ.
EA1	-1.99	0.988	220	-2.68	0.968	220
EA2	-1.91	0.570	220	-2.07	0.633	220
		0.513	121		0.472	121
		-0.625	022		-0.593	022
EPD	-5.91	0.691	220	-7.23	0.702	220
		-0.688	202		-0.610	202

S2.2 Effects of the LUMO+1 and higher MOs in the CISD active space

The choice of the level of calculation in the CISD active space also affects the results to some extent. We herein show that the present choice of CISD active space is reasonably good, and extending the space does not affect the qualitative aspects as a matter of fact. We compare the results from the active spaces (HOMO−67) – LUMO and (HOMO−4) – (LUMO+14), again for the ground electronic states of the key three states having a hole in EA1, EA2, or EPD, which are obtained by the same manner as in Section S1. The number of doubly-occupied MOs are different, but it hardly makes difference in electronic states, because the contribution of excited-state configuration from MOs lower than HOMO−1 are almost always zero for these three structures. The reason why we take a number of the lower MOs into account for the active space is to avoid computational difficulty caused by the MO level exchange between the active and frozen spaces along the dynamical path.

As shown in Tab. S1, the electronic states for the three key states that have a hole in EA1$^+$, EA2, or EPD would be regarded as qualitatively invariant by the choice of CISD active space, because the dominant configurations are all the same and the CI coefficients are similar to each other. One of the reasons why LUMO+1 and the higher MOs are not influential in the low-lying states is that the super molecular system is a cation as a whole. However, the energies are estimated to be different as much as 1 eV, which does not change the qualitative conclusions about the reaction mechanism.

References

[1] T. Yonehara, K. Hanasaki, and K. Takatsuka, *Chem. Rev.*, 2012, **112**, 499–542.

[2] K. Takatsuka, T. Yonehara, K. Hanasaki, and Y. Arasaki, *Chemical Theory Beyond the Born-Oppenheimer Paradigm: Nonadiabatic Electronic and Nuclear Dynamics in Chemical Reactions*, World Scientific, Singapore, 2015.

[3] K. Yamamoto and K. Takatsuka, *ChemPhysChem*, 2015, **16**, 2534–2537.

[4] K. Yamamoto and K. Takatsuka, *Chem. Phys.*, 2016, **475**, 39–53.

[5] K. Yamamoto and K. Takatsuka, *ChemPhysChem*, 2017, **18**, 537–548.

[6] K. Yamamoto and K. Takatsuka, *Phys. Chem. Chem. Phys.*, 2018.